Materials Research, Vol. 2, No. 3, 205-210, 1999.

Microstructural Evolution of the Al_2O_3-ZrO_2 Composite and its Correlation with Electrical Conductivity

Carlos A. Fortulan, Dulcina P.F. de Souza

Departamento de Engenharia de Materiais, UFSCar
C.P. 676, 13565-905 São Carlos - SP, Brazil

Received: August 15, 1998; Revised: March 30, 1999

The Al_2O_3-ZrO_2 composite was studied by impedance spectroscopy, a non destructive technique that was found to be sensitive to the composite's microstructure. The observed decrease in the zirconia grain and grain boundary conductivities points to compression on zirconia grain by alumina matrix. This effect increased with decreased concentration of zirconia in the composite. Measurements were taken of composites above the percolation threshold for vacancy conduction along the zirconia grains. The effect of densification and grain growth on the composite's conduction was measured. The changes in the zirconia grain and grain boundary specific conductivities were found to be correlated.

Keywords: *alumina - zirconia, electrical conductivity, microstructure*

1. Introduction

The alumina-zirconia composite, prepared by the introduction of fine ZrO_2 particles in the alumina matrix, has extensive structural applications owing to its excellent mechanical properties[1]. Through a suitable adjustment of the concentration of its components, this ceramic composite can show high standards of mechanical strength, toughness and hardness. Ceramic bodies made of pure alumina display properties of high hardness and good mechanical strength but poor toughness, while tetragonal zirconia has high mechanical strength, high toughness and lower hardness. The Al_2O_3-ZrO_2 composite offers the possibility of a compromise among these mechanical properties[2].

Low toughness is a typical mechanical property associated with glass and ceramic bodies, a behavior due to easy crack propagation. Ceramic matrix reinforcement has been considered as a potential tool for mechanical property improvement and increased reliability[3,4]. Two reinforcement mechanisms are considered in the literature: intrinsic and extrinsic. The later, which is more common, is the result of microstructural characteristics that inhibit crack propagation and protect the crack from the applied tension[5].

Mechanical strength is critically dependent on the microstructure, not only on the average microstructure, but also on its singularities. A sintered structural ceramic body must have a chemically and physically homogeneous microstructure and, in most common cases, high density, small grain size (around 3 μm) and narrow grain size distribution. This type of microstructure can be produced by low temperature sintering of chemical and physical homogeneous green compact[6].

Structural ceramic composites have rarely been electrically characterized because their electrical properties have no known applications. However, using the impedance spectroscopy technique, information can be obtained on microstructural homogeneity, grain boundary thickness changes and heat treatment effects[1,7]. Considering the Al_2O_3-ZrO_2 composite, an impedance spectroscopy analysis can provide information about the bulk without the mechanical disturbances introduced by the preparation process for SEM analysis.

The electrical conductivity of alumina grains in the Al_2O_3-ZrO_2 composite is several orders of magnitude smaller than that of the tetragonal zirconia. Therefore, in a low zirconia concentration, the composite acts as an insulator. The percolation threshold in this system will occur for spherical particle volumetric fractions equal to 16%. Above 22%, almost all the percolation paths are interconnected[8,9]. Figure 1 illustrates this behavior. Thus, above the threshold limit, the electrical conductivity of the composite is attributable to the zirconia percolation paths. This paper analyzes some experimental results on the electrical conductivity of this composite according to its microstructural evolution.

e-mail: dulcina@power.ufscar.br

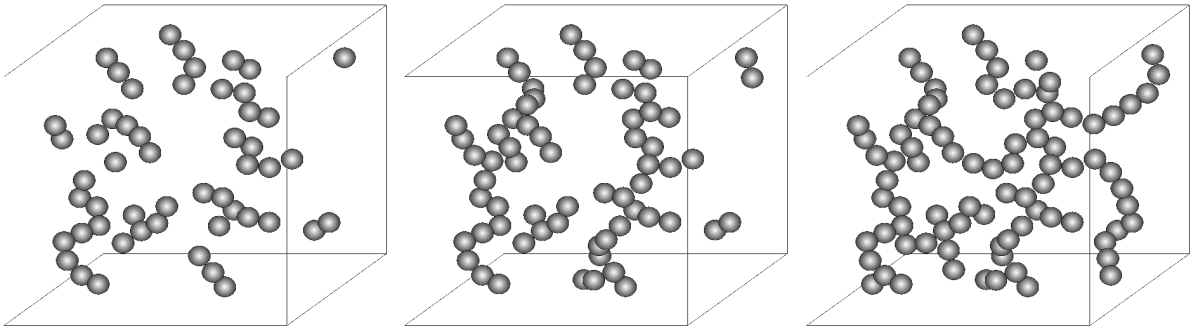

Figure 1. Schematic illustration of critical volume fraction in the percolative network of spherical inclusions in the random distribution: a) without percolation; b) critical volume fraction percolative network; c) percolative network cluster.

2. Experimental

The starting powders used to produce the composite pellets were alumina A16 (Alcoa, USA) and tetragonal zirconia TZ3Y (Tosoh, Japan), whose average particle sizes are 0.5 and 0.3 μm, respectively. The volumetric zirconia concentration used was 0, 10, 20, 30, 50, and 100, which is pure zirconia, and the samples were labeled A0, A10, A20, A50 and A100, respectively. Mixing of the starting powders was done in a high-density polyethylene mill using YTZ ceramic balls (Tosoh, Japan) in water, with ammonium polyacrylate as the dispersing agent. After 16 h mixing, 2 wt% of polyvinyl alcohol and 0.8 wt% of ethylene glycol were added. After drying, the powder was screened in an 80 mesh sieve. Pellets were isostatically pressed at 210 MPa and sintered in the 1450 to 1600 °C range. The density of the sintered samples was measured using the Archimedes method. SEM (ZEISS 9600, Germany) microstructure studies were made of pellets with 1 μm grit diamond paste final polishing and thermally etched 100 °C below the sintering temperature for 5 min. The average grain size was obtained using the standard method ASTM E 112-84 applying statistical correction for the volumetric concentration of each phase. Impedance spectroscopy measurements (HP 4192 A), of pellets of 17 mm diameter and 2.5 mm thickness, were made with platinum electrodes (DEMETRON 308 A platinum paste) in the frequency range of 5 Hz to 13 MHz from 300 to 500 °C. The spectra analyses were made using a specific software[10].

3. Results and Discussion

Microstructures of the 1600 °C - 2 h sintered pellets of compositions A0, A10, A20, A30, A50 and A100 are shown in Fig. 2. The A20 composition microstructure shows zirconia grains with a different contrast, and even gets images from secondary electrons.

The average zirconia grain size in all the 1600 °C - 2.0 h sintered samples was constant, *i.e.*, around 0.7 μm, while the alumina grains are larger for the A0 composition in comparison to the others, with their average grain size decreasing as the zirconia concentration increases, Table 1. The same table shows a small variation in density values compared to the theoretical values among all the samples. Hence, adding zirconia inhibits alumina grain growth and, when the addition of zirconia exceeds 30 vol.%, this effect is kept constant.

Due to its volumetric characteristic, the onset of percolation in these composites cannot be observed in the microstructures. The best technique for this purpose is to measure the electrical conductivity. As expected, the A10 sample is an insulator. Figure 3 shows the impedance plots of samples A20 to A100 sintered at 1600 °C - 1 h. Two well defined arcs are displayed by all samples; the left arc is the result of grain conductivity while right one, with a longer relaxation time, is due to the less conductive grain boundary. The grain and grain boundary resistances decrease,

Table 1. Alumina grain size and apparent density after sintering at 1600 °C - 2 h.

Composition	A0	A10	A20	A30	A50
Alumina grain size (μm)	3.2	1.7	1.4	1.3	1.3
Apparent density (g/cm^3)	3.91	4.07	4.33	4.56	4.99
(% theoretical density)*	(98.2)	(97.1)	(98.4)	(98.9)	(99.2)

* The theoretical densities were calculated from full density of α-alumina, 3,98 g/cm^3, and zirconia TZ3Y, 6,08 g/cm^3, [11,12] and their volumetric fraction.

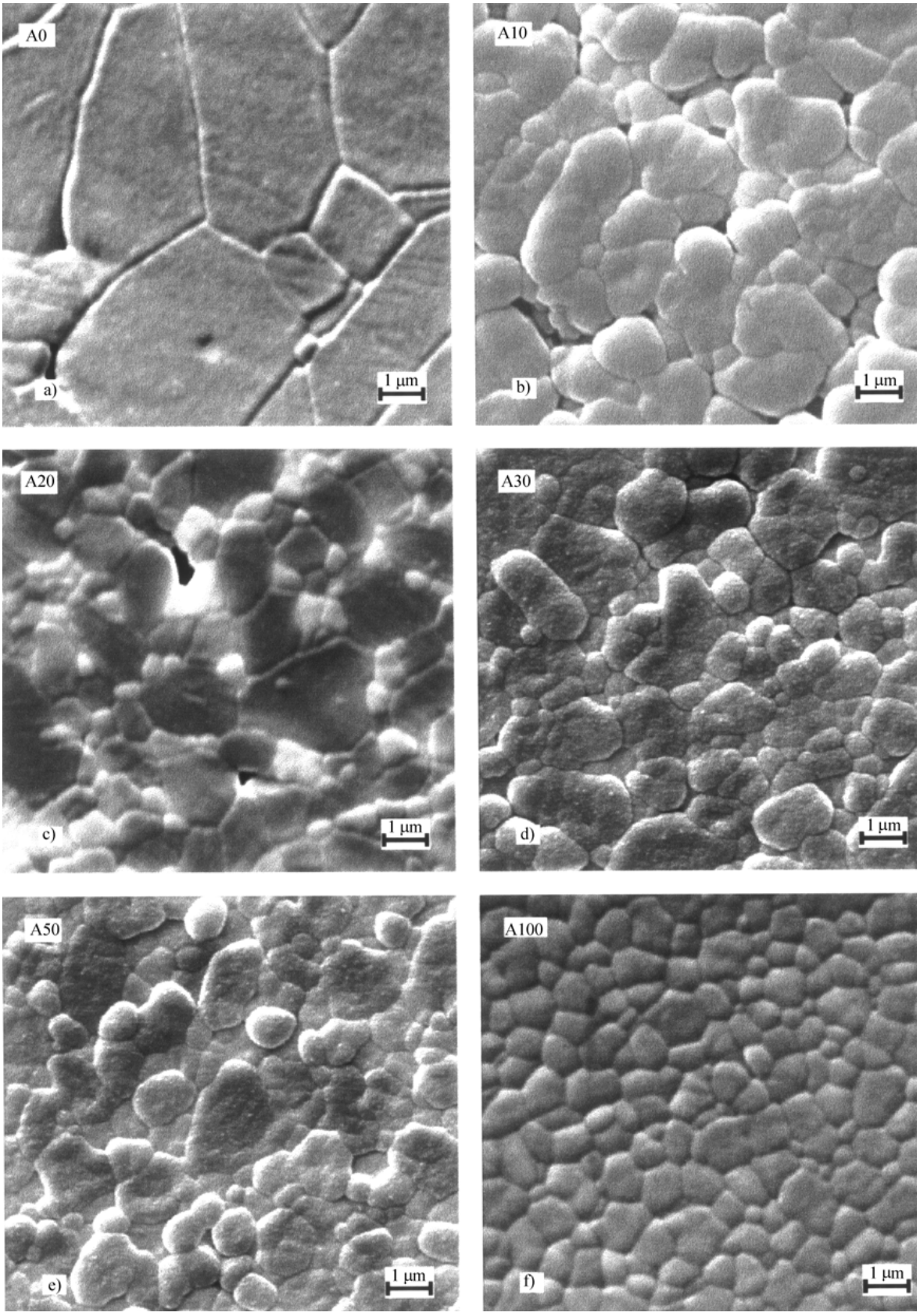

Figure 2. Microstructural evolution followed by SEM, 30 KV, (secondary electrons) of the compositions A0, A10, A20, A30, A50 and A100, sintered at 1600 °C for 2 h.

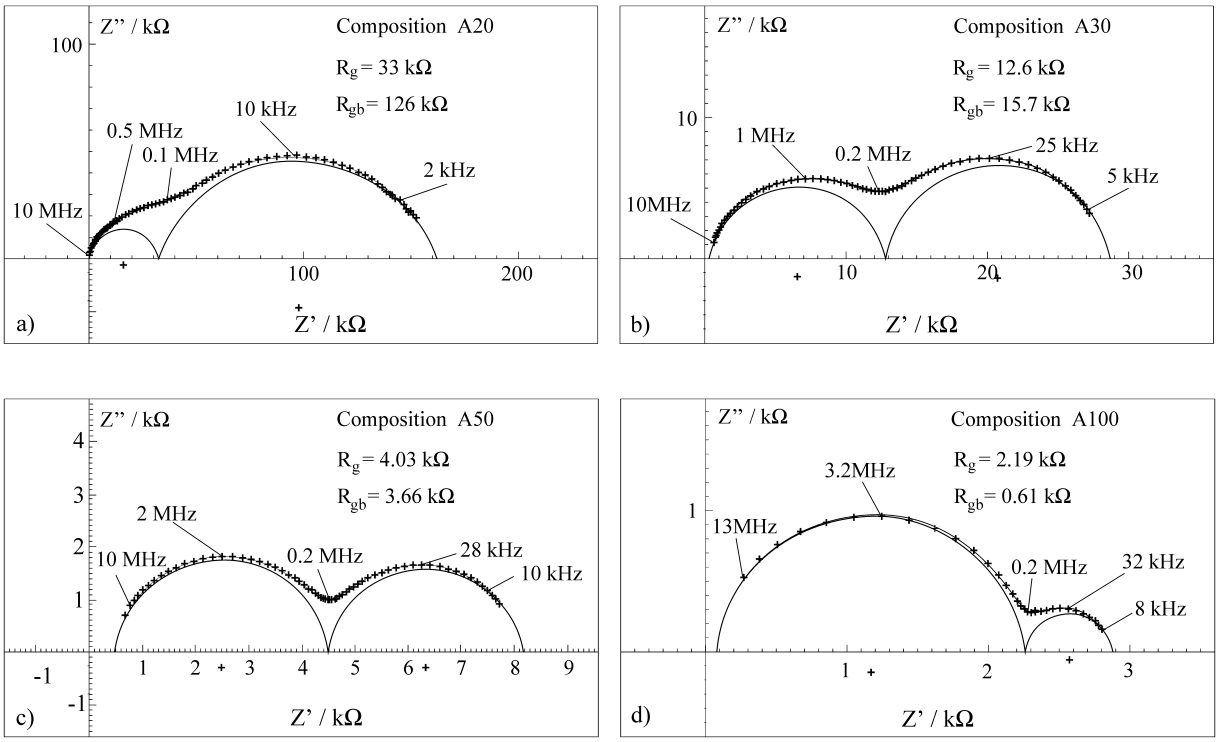

Figure 3. Complex impedance plots recorded at 400 °C for the compositions sintered at 1600 °C - 2 h: a) A20; b) A30; c) A50; d) A100.

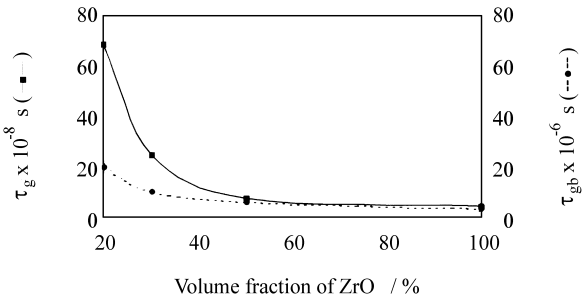

Figure 4. Relaxation time for the grain (τ_g) and the grain boundary (τ_{gb}) with zirconia concentration for sintered samples at 1600 ºC - 2 h and recorded at 400 °C.

raising the concentration of zirconia, since the number of percolation paths increase with the zirconia concentration. This is a general statement requiring knowledge of the specific grain σ_g^{sp} and grain boundary σ_{gb}^{sp} conductivity to become quantitative. The measured relaxation time is related with specific conductivity by:

$$\tau = \varepsilon_0 \frac{\varepsilon}{\sigma^{sp}}$$

where τ is the measured relaxation time, ε_o is the vacuum permitivity, ε is the ziconia dielectric constant, and σ^{sp} is the zirconia specific conductivity. Therefore, the relaxation time is an intrinsic material property that is shorter for higher conductive materials and is independent of the particular mode of percolation or any particular geometrical organization of the material[13]. The complex

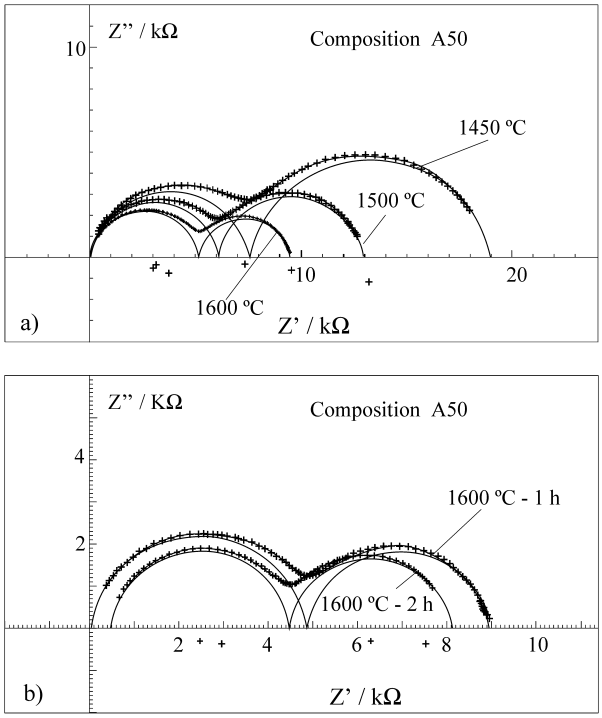

Figure 5. AC impedance plots recorded at 400 °C for composition A50 sintered in the following conditions: a) 1450 °C, 1500 °C and 1600 °C for 1 h; b) 1600 °C - 1 h and 1600 °C - 2 h.

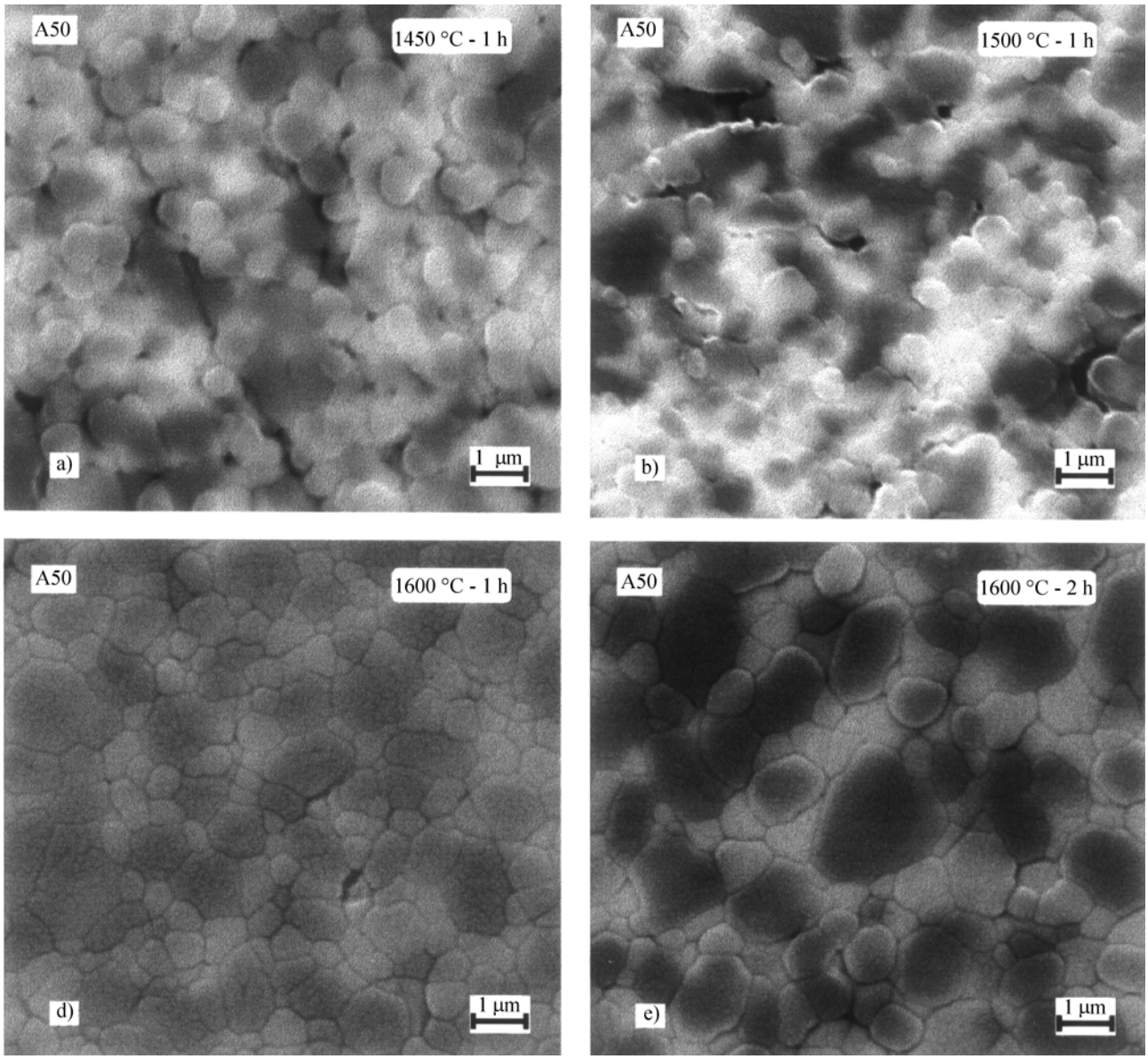

Figure 6. Microstructural evolution followed by SEM, 30 KV, (backscattered electrons) of the composition A50 with the sintering temperature.

impedance plots refer only to the conduction paths of zirconia because alumina conductivity is several orders of magnitude lower. Figure 4 shows the dependence of relaxation time on the zirconia concentration obtained from the impedance plots shown in Fig. 3. These results show that grain and grain boundary specific conductivity increases as the zirconia concentration is increased and is kept nearly constant above a 50 vol.% zirconia concentration, or, conversely, specific conductivity decreases progressively as the zirconia concentration decreases, *i.e.*, zirconia in alumina becomes less conductive. This effect is more pronounced for the grain conductivity. The zirconia grain in sample A20 is 15 times less conductive than in sample A100. This behavior can be understood as being due to the pressure exerted on the zirconia owing to alumina shrinking in the sintering. The simultaneous decrease in the grain boundary conductivity, although smaller, indicates how the grain and grain boundary conductivities are linked together.

Figure 5 shows how the impedance plot changes with sintering temperature for 1 h sintering time, Fig. 5A, and with sintering time at 1600 °C, Fig. 5B. Sintering at 1450 °C of sample A50 results in samples with large depressed angles in the grain and grain boundary impedance plot. Increasing the sintering temperature decreases the depressed angle. Spread in relaxation time among all the grains causes a depressed semi circle. Because densification increases sample homogeneity by the elimination of pores, the stress tends to be same on all the zirconia grains; consequently, the depressed angle decreases. We are con-

Table 2. Relaxation time for the grain and the grain boundary for composition A50 recorded at 400 °C.

Sintering	Density	Relaxation time	
Temp. - time	g/cm^3 (D_{ap}/D_{th})	Grain (10^{-8} s)	Grain boundary (10^{-6} s)
1450 °C - 1 h	4.52 (87.6)	10.6	6.6
1500 °C - 1 h	4.77 (92.4)	9.3	6.2
1600 °C - 1 h	4.97 (96.3)	8.0	6.2
1600 °C - 2 h	4.99 (96.7)	8.0	6.5

fident of the accuracy of our statement regarding the relationship between the depressed angle and the spread in the relaxation time because we carried out analyses of electrical circuits with programmed variations of the RC product that resulted in the depressed semi circle[14]. Another experimental finding is the decrease of the sample grain and grain boundary electrical resistance due to densification and, to a lesser extent, due to alumina grain growth. The main cause of this effect is attributed to the increase in the number of percolation paths as a result of the decresed volume available to the zirconia grains. Table 2 shows that densification decreases relaxation times, *i.e.*, it increases conductivity, as has already been shown in Fig. 3. Figure 6 indicates the microstructural evolution of the same samples of A50 composition used to obtain the impedance plots shown in Fig. 5.

4. Conclusions

The electrical behavior of the grain and grain boundary conductivity of tetragonal zirconia in the Al_2O_3-ZrO_2 composite was measured above the threshold concentration of zirconia for electric current percolation. It was found that zirconia grain and grain boundary specific conductivities are very sensitive to the pressure exerted by the alumina on the zirconia grains. The pressure on the zirconia grains is ascribed to alumina shrinkage during sintering. The smaller the concentration of zirconia, the stronger this effect. Experimentally, this effect shows up in the grain and grain boundary relaxation time. The behavior of the relaxation time with sintering temperature for samples of the same composition soaked for 1 h indicates that grain specific conductivity increases when the apparent density increases. Densification also increases sample homogeneity. Homogeneous samples have a low spread in the relaxation times, expressed in the impedance plots by a small depressed angle.

The simultaneous grain and grain boundary changes in the relaxation time under the internal stress bring into focus the contribution of the space charge, located in the grain interface, though inside the grain, to grain boundary conductivity.

Acknowledgments

The authors acknowledge the Brazilian financing agency CNPq for the grants supporting this work.

References

1. Osendi, M.I.; Jurado, J.R. *Zirconia'88 – Advances in zirconia science and technology*, p. 239-249, 1988.
2. Burelli, M.; Maschio, S.; Meriani, S. *Journal of Materials Science*, v. 33, p. 441-444, 1988.
3. Richerson, D.W. *Modern ceramic engineering, Properties, processing and use in design*, 1992.
4. Zanotto, E.D.; Migliore Jr, A.R. *Cerâmica*, v. 37, n. 247, p. 7-16, 1991.
5. Hannink, R.H.J.; Gross, V.; Muddle, B.C. *Ceramics International*, v. 24, p. 45-51, 1998.
6. Ting, J.-M.; Lin, R.Y. *Journal of Materials Science*, v. 29, p. 1867-1872, 1994.
7. Gerhardt, R. *Ceramic Engineering/Science proceedings*, n. 10, p. 1174-1181, 1994.
8. Balberg, I.; Binenbaum, N. *Phys. Ver. B, Condens. Matter,* v. 35, n. 16, p. 8749-52, 1987.
9. Lange, F.F.; Atteraas, L.; Zok, F. *Acta Metall. Mater.,* v. 39, n. 2, p. 209-19, 1991.
10. Levy, M. "Spect" Software, Laboratoire d'Eletrochimie et de Physicochimie des Matériaux et des Interfaces - LEPMI/INPG - Grenoble - France, 1993.
11. Gitzen, W.H. *Alumina as a Ceramic Materials* , p. 31, AcerS.
12. Ingel, R.P.; Lewis III, D. *J. Am. Ceram. Soc.,* v. 69 n. 4, p. 325-32, 1986.
13. Souza, M.F. de; Souza, D.P.F. de *Radiation Effects & Defects in Solids,* v. 146, p. 215-227, 1998.
14. Souza, M.F. de; Vilanova, R.P.; Souza, D.P.F. de *unpublished work.*